Virology 527 (2019) 38–46

Contents lists available at ScienceDirect

Virology

journal homepage: www.elsevier.com/locate/virology

Role of *Tobacco vein banding mosaic virus* 3′-UTR on virus systemic infection in tobacco

Ying Wang[a,b,c,1], Zheng-You Yang[b,1], Yan-Ping Tian[a,1], Chao Geng[a], Xue-Feng Yuan[a,*], Xiang-Dong Li[a,*]

[a] Department of Plant Pathology, College of Plant Protection, Shandong Agricultural University; Shandong Province Key Laboratory of Agricultural Microbiology, Tai'an 271018, PR China
[b] Department of Microbiology, College of Life Sciences, Shandong Agricultural University, Tai'an 271018, PR China
[c] College of Life Sciences, Linyi University, Linyi 276005, PR China

ARTICLE INFO

Keywords:
3'-UTR
Movement
Potyvirus
Systemic infection
Tobacco vein banding mosaic virus

ABSTRACT

To investigate the role of *Tobacco vein banding mosaic virus* (TVBMV) 3′-UTR in virus systemic infection, three types of deletions were introduced into TVBMV infectious clone pCaTVBMV-GFP. Mutants with deletions at the nucleotide position 8–42, 43–141, or 163–174 in the 3'-UTR failed to cause systemic infection in *N. benthamiana* plants. Other deletion mutants caused delayed systemic infection and milder vein clearing and mosaic symptoms. Most progeny mutant virus had acquired nucleotides, similar to or different from the deleted nucleotide sequences, after a single passage in the host plant. Nucleotides at the position 8–42 near the 5′-terminus of TVBMV 3′-UTR could form a stem-loop (SL) like structure which was crucial for TVBMV systemic movement in tobacco. We proposed that this SL like structure, and thus 3′-UTR, has an essential role in TVBMV systemic infection.

1. Introduction

To establish infection in plant, virus needs to replicate in initially inoculated cells, moves between cells and then to other parts of the host plant. In addition to virus replication- and virus movement-associated proteins, the 3′-untranslated region (3′-UTR) of virus genomic RNA was also reported to be important in virus infection (Iwakawa et al., 2007; Dong et al., 2015; Shwetha et al., 2015). A recent study has indicated that disruption of a stem-loop (SL) like structure in the coat protein (CP) gene or in the 3′-UTR of *Tobacco mosaic virus* (TMV) enhanced TMV replication (Guo and Wong, 2018). An earlier report had indicated that a region in the 3′-UTR of dengue virus could enhance dengue virus replication in Baby Hamster Syrian Kidney-21 but not in mosquito cells (Alvarez et al., 2005). Serial deletions made in the 3′-terminal genome of *Dengue virus type 2* affected virus accumulation in mammalian cells (Teramoto et al., 2008). Yun and other reported that deletion of 381 nucleotides (nt) from the 5'-terminus of *Japanese encephalitis virus* 3′-UTR had no significant effect on virus replication (Yun et al., 2009). The above studies promoted us to investigate the importance of *Tobacco vein banding mosaic virus* (TVBMV) 3′-UTR on virus replication in its host plant.

Several mechanisms, including RNA recombination, primer-mediated sequence repair, viral replicase terminal nucleotidyl transferase activity and multiple host cellular proteins, have been reported to protect the terminal sequences of viral genomic RNAs (Bienz et al., 1992; Bol, 2005; Dreher, 2009; Garnier et al., 1986; Mackenzie et al., 1998; Skuzeski et al., 1996). It was reported that progeny mutant virus RNAs could be repaired by addition of various length sequences at the original deletion loci. Examples of virus terminal sequence repair included *Cucumber mosaic virus* (CMV) satellite RNA (Burgyan and Garcia-Arenal, 1998; Kwon et al., 2014), *Turnip crinkle virus* (TCV) satellite RNA (Guan and Simon, 2000) and *Dengue virus type 2* (Teramoto et al., 2008).

Tobacco vein banding mosaic virus (TVBMV) is a species in the genus *Potyvirus*, family *Potyviridae* and often causes significant economic losses to solanaceous crops (Tian et al., 2007). TVBMV genome is a positive-strand RNA with about 9600 nucleotides (nt) and poly (A) tail. The 5'- and 3'-untranslated regions (UTRs) of TVBMV contain 171 and 184 nt, respectively. Like other potyviruses, TVBMV genomic RNA has two open reading frames (ORFs). The large ORF encodes a polyprotein that can be cleaved into ten mature proteins (ie P1, HC-Pro, P3, 6K1, CI, 6K2, NIa-Pro, VPg, NIb and CP) by three TBVMV-encoded proteinases.

* Corresponding authors.
E-mail addresses: yuanxf@sdau.edu.cn (X.-F. Yuan), xdongli@sdau.edu.cn (X.-D. Li).
[1] These authors contributed equally.

https://doi.org/10.1016/j.virol.2018.11.001
Received 23 July 2018; Received in revised form 31 October 2018; Accepted 1 November 2018
Available online 16 November 2018
0042-6822/

The small ORF encodes P1, HC-Pro and P3N-PIPO that is translated from the region within the P3-encoding sequence through a transcriptional frame shifting strategy (Chung et al., 2008; Geng et al., 2015).

Functions of 3′-UTRs of potyviruses are largely unknown. A 3′-terminal poly(A) deletion mutant of *Clover yellow vein virus* (ClYVV) was reported to be repaired during its infection in plant (Tacahashi and Uyeda, 1999). In a different study ClYVV mutants lacking various regions of its 3′-UTR were unable to cause infection in its broad bean host (Sekiguchi et al., 2003). In this study, we introduced different length deletions into a TVBMV infectious clone (pCaTVBMV-GFP) (Gao et al., 2012; Geng et al., 2015) at the viral 3'-end region through site-directed mutagenesis and analyzed their systemic infection in *Nicotiana benthamiana* plants.

2. Material and methods

2.1. Deletion mutagenesis

Primer 3-1-20-F and 3-1-20-R were designed using the strategy described by Liu and Naismith (2008) and used to introduce a 20 nt deletion in the 5′ end terminal region in the 3′-UTR of the full-length TVBMV infectious clone (pCaTVBMV-GFP) described previously (Geng et a;., 2015). High fidelity Phusion DNA polymerase (Thermo, Finland) was used during the over-lapping PCR. Restriction enzyme *Dpn* I was incubated with the PCR product at 37 °C for 60 min to remove the original plasmid sequence. The resulting PCR product was transformed into *Escherichia coli* cells (JM109) by the heat-shock treatment. Same approach was also used to construct other mutants with specific deletions in the TVBMV 3′-UTR: 3′-Δ1–60, 3′-Δ8–42, 3′-Δ8–14, 3′-Δ15–35, 3′-Δ36–42, 3′-Δ43–60, 3′-Δ61–100, 3′-Δ101–141, 3′-Δ142–162, 3′-Δ163–174, 3′-Δ184, 3′-Δ183–184, 3′-Δ181–184, 3′-Δ178–184, 3′-Δ175–184 and 3′-Δ165–184. All the constructs were sequenced to confirm the intended deletions. All the primers used for the mutagenesis, PCR amplification, and plasmid sequencing are listed in the Supplemental Table 1.

Two primer pairs (3-1-20/14nt^{Ins}-F and 3-1-20/14nt^{Ins}-R), each carrying an inserted 14-nt sequence, and two primer pairs (3-15-35/35nt^{Ins}-F and 3-15-35/35nt^{Ins}-R), each carrying an inserted 35-nt sequence, were used to construct mutant plasmids 3′-Δ1–20/14nt^{Ins} and 3′-Δ15–35/35nt^{Ins} by a one-step site-directed insertion mutagenesis protocol (Liu and Naismith, 2008).

2.2. Growth of test plants

Seeds of *N. benthamiana* plants was sown in soil. The seedlings at the 3–4 leaf stage were transplanted individually into pots and grown in inside a growth chamber set at 25 ℃ and a 16 h / 8 h (light/dark) photoperiod.

2.3. Inoculation and fluorescence visualization

Plasmid pCaTVBMV-GFP and its mutant plasmids were transformed individually into *Agrobacterium tumefaciens* GV3101 cells following a freeze and thaw transformation procedure (Cui et al., 1995). After overnight culturing, *Agrobacterium* cultures were pelleted through centrifugation at 5 000*g* for 3 min, the pellets were resuspended individually in an induction solution (10 mmol/L MES, pH5.8, 0.1 mmol/L acetosyringone and 10 mmol/L $MgCl_2$), and incubated for 3 h at room temperature. Leaves of *N. benthamiana* plants at the 5–6 leaf stage were infiltrated with an *A. tumefaciens* GV3101 culture harboring a *gfp* gene expression vector (OD_{600} = 0.5) using needle-less syringes. At three days post agro-infiltration (dpai), the agro-infiltrated plants were examined for GFP expression under a hand-held UV (365 nm wavelength) lamp Blak-Ray B100-AP lamp, UV products, Upland, CA91786, USA).

2.4. RNA extraction, sequencing and qRT-PCR

Total RNA was extracted from agro-infiltrated *N. benthamiana* plant leaves using a Mini-RNA kit (Qiagen, Germany). TVBMV cDNA was made using primer 1985-3-R and a *Moloney Murine leukemia virus* (M-MuLV) reverse transcriptase (TransGen, China). PCR amplifications were performed using primer TVBMV-9458-F and 1985-3-R, and a Phusion DNA Polymerase (Thermo, Finland). The resulting amplicons were cloned and sequenced using ABI3730 sequencer by Shanghai Biosune Biotechnology Company (Shanghai, China).

The accumulation levels of TVBMV-GFP RNA and its mutants were determined using qRT-PCR. For each sample, the first-strand cDNA was synthesized using 100 ng total RNA, M-MuLV reverse transcriptase and primer 1985-3-R. The reverse transcription reaction was carried out at 42 ℃ for 60 min and 2 μL cDNA was used in each qPCR reaction. The qRT-PCR was done using a Power SYBR green PCR master mix as instructed (TaKaRa, Japan) on an ABI Prism 7500 Fast sequence detection system. The expression level of elongation factor 1α (EF1α) gene was used as the internal control. The reaction conditions of qPCR were as 95 ℃ for 2 min; 45 cycles of 5 s at 95 ℃, 30 s at 58 ℃, 30 s at 68 ℃; 3 min at 68 ℃; and 30 s at 55–95 ℃. The TVBMV sequence was amplified using primer TVBMV-qCP-636-F and TVBMV-qCP-728-R. The EF1α gene was amplified using primer EF1α-F and EF1α-R. Statistical analyses were done using the unpaired two-sample test (two-tailed) (Schmittgen et al., 2000; Winer et al., 1999).

2.5. RNA secondary structure analysis

The secondary structures in the WT or mutant TVBMV genome sequences were predicted using the Mfold program at the website (http://unafold.rna.albany.edu/?q=mfold/RNA-Folding-Form) (Zuker, 2003), and illustrated using the Photoshop CS3 (Adobe Systems Incorporated). Because the full length TVBMV genome RNA has 9648 nt, longer than the sequence length limit that the Mfold can process, a 900 nt region, ranging from nucleotide position 5401 to 6300 of TVBMV genomic RNA was excluded for the analysis of secondary structures in the 3′-UTR sequence.

3. Results

3.1. Deletion of specific sequence from TVBMV 3′-UTR affected virus systemic infection in N. benthamiana plants

To determine the effect of TVBMV 3′-UTR on virus systemic infection in *N. benthamiana* plants, we introduced three different types of deletion/insertion mutations into a previously reported infectious pCaTVBMV-GFP clone.

The first mutant group contained various deletions in the 5′-end region of TVBMV 3′-UTR (Fig. 1A). After these mutant constructs were transformed individually into *Agrobacterium* cells, the *Agrobacterium* cultures were infiltrated individually into *N. benthamiana* leaves. At 11 dpai, the plants agro-infiltrated with the WT TVBMV-GFP (pCaTVBMV-GFP) showed severe mosaic in their systemic leaves and strong green fluorescence in both infiltrated and systemic leaves under the UV illumination (Fig. 1B). Mutant 3′-Δ1–20 had a 20 nt deletion at the 5′-end of the 3′-UTR and caused vein clearing and weak green fluorescence in systemic leaves. In contrast, mutant 3′-Δ1–60 had a 60 nt deletion at the 5′-end of the 3′-UTR and failed to cause any virus like symptoms and green fluorescence in the infiltrated plants (Fig. 1B; upper panel). We then analyzed more TVBMV 3′-UTR deletion mutants (i.e., 3′-Δ8–14, 3′-Δ15–35, 3′-Δ36–42, and 3′-Δ8–42) and the results showed that the mutant 3′-Δ8–14, 3′-Δ15–35 and 3′-Δ36–42 were able to induce weaker green fluorescence in systemic leaves but not the mutant 3′-Δ8–42 (Fig. 1B; lower panel).

Analyses of viral RNA accumulations in systemic leaves through qRT-PCR showed that the accumulation levels of viral RNA agreed with

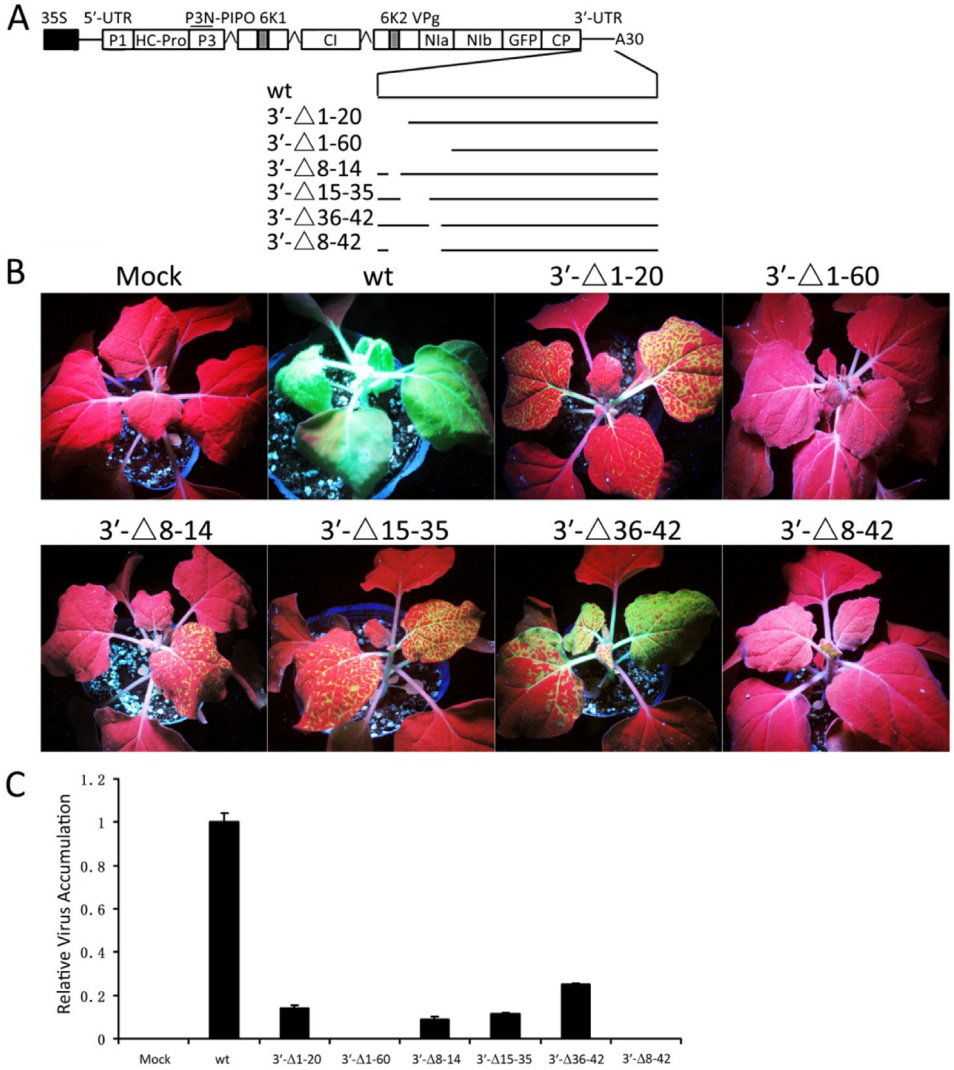

Fig. 1. Effects of 5′-terminal deletions in 3′-UTR on systemic movement of TVBMV. A, Schematic diagram of 5′-end mutants in the 3′-UTR of TVBMV. B, Green fluorescence in *Nicotiana benthamiana* plants inoculated with different constructs at 11 dpi under UV light. C, Relative RNA accumulation in systemically infected leaves through qRT-PCR at 11 dpi.

the results of symptom observation (Fig. 1C). The accumulation levels of viral RNA in the plants infiltrated with mutant 3′-Δ1–20, 3′-Δ8–14, 3′-Δ15–35 or 3′-Δ36–42 were all less than 30% of that in the plants infiltrated with the WT pCaTVBMV-GFP (Fig. 1C). Plants infiltrated with mutant 3′-Δ1–60 or 3′-Δ8–42 did not accumulate TVBMV RNA and thus did not show any virus like symptoms.

The second mutant group contained five mutants with the deletions in the middle region of the 3′-UTR (Fig. 2A). The mutant 3′-Δ142–162 induced similar virus symptoms shown by the plants infiltrated with the WT pCaTVBMV-GFP (Fig. 2B). Mutant 3′-Δ43–60, 3′-Δ61–100, 3′-Δ101–141 and 3′-Δ163–174 failed to cause any virus like symptoms and green fluorescence in the infiltrated leaves by 4 dpai (Fig. 2B). Result of qRT-PCR showed that the accumulation level of TVBMV RNA in the plants infiltrated with mutant 3′-Δ142–162 was about 55% of that in the plants infiltrated with the WT pCaTVBMV-GFP. No TVBMV RNA was detected by qRT-PCR in the systemic leaves of the *N. benthamiana* plants infiltrated with mutant 3′-Δ43–60, 3′-Δ61–100, 3′-Δ101–141 or 3′-Δ163–174 (Fig. 2C), indicating that nt 43–141 or 163–174 are important for TVBMV systemic movement in *N. benthamiana* plants while nt 142–162 is dispensable.

The third mutant group contained six mutants with deletions near the 3′-end of the 3′-UTR (Fig. 3A). Like the WT virus, mutant 3′-Δ184 and 3′-Δ183–184 caused mild mosaic and strong green fluorescence in systemic leaves of *N. benthamiana* by 4 dpai (Fig. 3B, upper panel). By 11 dpai, the plants infiltrated with the WT pCaTVBMV-GFP, mutant 3′-Δ184, 3′-Δ183–184 or 3′-Δ181–184 showed plant stunting and leaf epinasty, and strong green fluorescence. The plants infiltrated with mutant 3′-Δ178–184 or 3′-Δ175–184 showed milder disease symptoms and green fluorescence. The plants infiltrated with mutant 3′-Δ165–184 did not show virus like symptoms and green fluorescence by 11 dpai (Fig. 3B, lower panel). Results of qRT-PCR showed that the accumulation levels of viral RNA in the systemic leaves of the plants infiltrated with mutant 3′-Δ184, 3′-Δ183–184, 3′-Δ181–184, 3′-Δ178–184 or 3′-Δ175–184 agreed with the symptom development in these plants. No viral RNA was detected in the plants infiltrated with the mutant 3′-Δ165–184 (Fig. 3C), indicating that deletion of the last four to ten nucleotides from the 3′-end genome delayed viral systemic infection, and deletion of 20 nt from the 3′-end genome abolished the systemic infection of TVBMV.

3.2. 3′-UTR sequences of progeny viral RNAs are different from that of the parental virus

To investigate the genetic variation of TVBMV 3′-UTR, we sequenced the 3′-UTR region of progeny viral RNAs representing the WT or mutant TVBMV. Results showed that, of the 23 sequenced clones

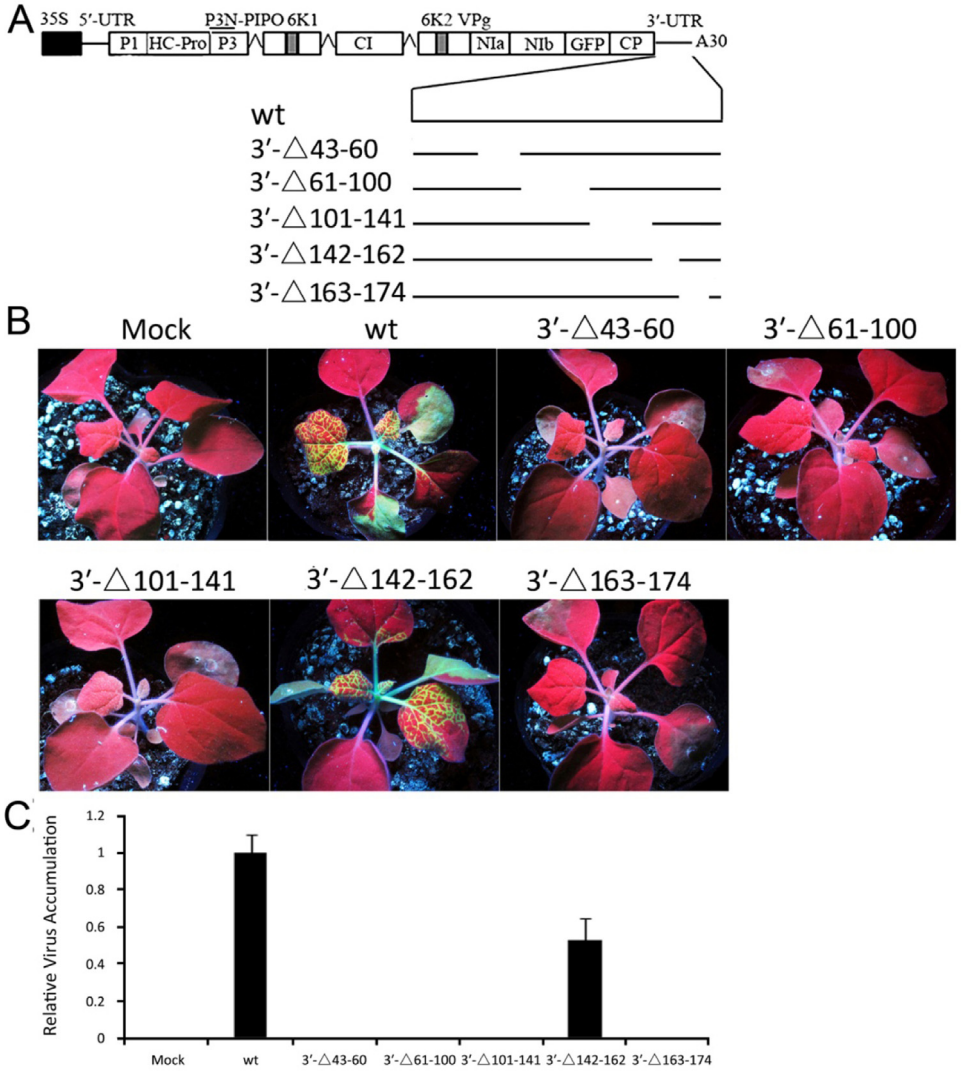

Fig. 2. Effects of internal deletions in TVBMV 3′-UTR on systemic movement of TVBMV. A, Schematic diagram of internal deletion mutants in 3′-UTR of TVBMV. B, Green fluorescence in different mutants-inoculated *Nicotiana benthamiana* plants at 4 dpi under UV light. C, Relative RNA accumulation in systemically infected leaves by qRT-PCR at 4 dpi.

representing the WT TVBMV, six clones were terminated with GAGGG, same as the parental virus sequence, fifteen clones were ended with GAGG and two clones had a deletion of four nucleotides (Fig. 4A), indicating that the 3'-UTR of TVBMV genomic RNA was continuously under the pressure to change. A total of nineteen clones were obtained from the plants infiltrated with the mutant 3′-Δ184 and 18 of them had the identical sequences as the mutant vector sequence. One clone had a deletion of GAGG before the poly A tail. Seventeen clones were obtained from the plants infiltrated with the mutant 3′-Δ183–184 and all of them had acquired a G at the original deletion site. Sixteen clones were obtained from the plants infiltrated with the mutant 3′-Δ181–184 and 15 clones had an insertion of agg at the original deletion site. One clone had an additional g deletion to yield a final deletion of gagg. The results suggest that most progeny viral RNA with 2 or 4 nt deletion at the 3′-UTR can be restored to the WT sequences.

Eleven clones were obtained from the plants infiltrated with the mutant 3′-Δ178–184 and three clones were restored to the original sequences. Eight clones had nucleotide changes at the original deletion site but the new sequences were all different from the WT TVBMV sequence. Twenty-one clones were obtained from the plants infiltrated with the mutant 3′-Δ175–184 and three clones were mutated to have the same nucleotide length as the parental virus. Nine clones had acquired 11 nucleotides and other nine clones had a deletion of G followed by an addition of 11 nucleotides, resulting the same sequence length at this position as that of the WT TVBMV. However, the new sequences were different from the WT TVBMV, even though all the new sequences were terminated with GGG (Fig. 4A). Taken together, we conclude that the mutant progeny RNAs can restore sequence length through random acquisition of nucleotides.

For mutants with deletions at the 5′-end of the 3′-UTR, additions of nucleotides were also observed at the original deletion site. For example, 13 clones were obtained from the plants infiltrated with the mutant 3′-Δ1–20 and all of them had acquired 14 nt at the original deletion site. It is noteworthy that 12 of the 14 acquired nucleotides (tattatagtgta) were identical to that at the nucleotide position 31–43 in the WT 3′-UTR (Fig. 4B). Ten clones were obtained from the plants infiltrated with the mutant 3′-Δ8–14 and all the clones had their seven deleted nucleotides restored. Fifteen clones were obtained from the plants infiltrated with the mutant 3′-Δ36–42 and ten clones had their deleted sequence restored perfectly. The other five clones acquired eight nucleotides that was a duplication of the downstream sequence (underlined). Nine clones were obtained from the plants infiltrated with the mutant 3′-Δ15–35 and all the clones had a 35 nt insertion at the original deletion site. Within the inserted sequences, 33 nt (underlined)

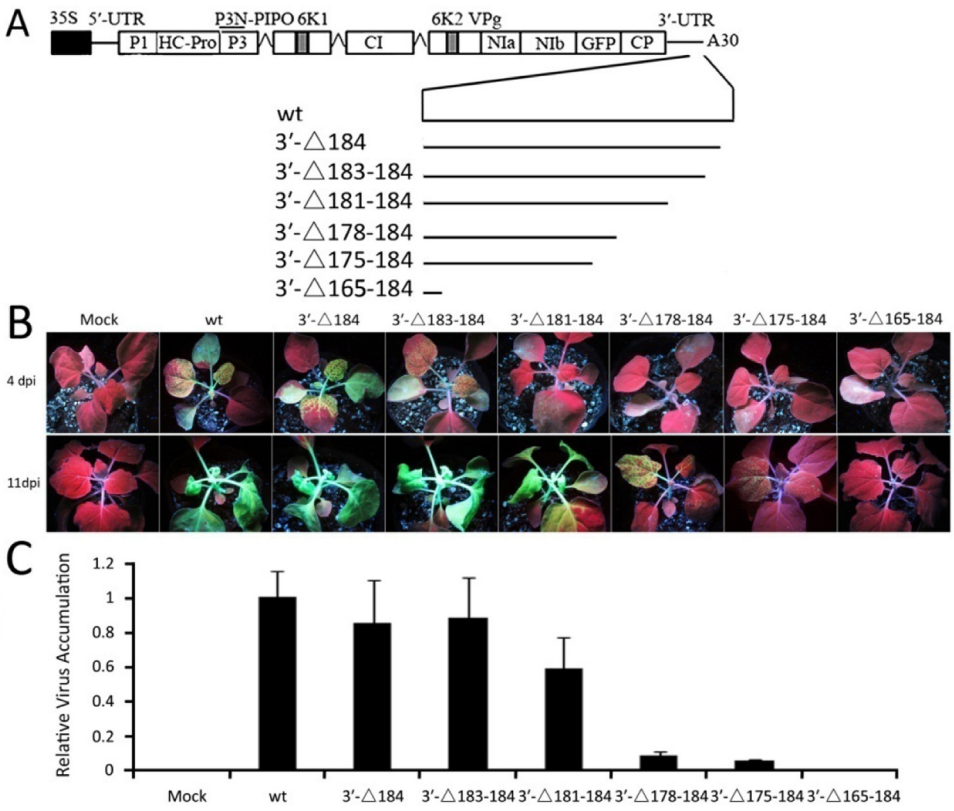

Fig. 3. Effects of 3′-terminal serial deletions in TVBMV 3′-UTR on systemic movement of TVBMV. A, Schematic diagram of 3′-terminus deletion mutants in TVBMV genome. B, Green fluorescence under UV light in different mutants-inoculated *Nicotiana benthamiana* plants at 4 and 11 dpi. C, Relative RNA accumulation in systemically infected leaves by qRT-PCR at 11 dpi.

were identical to the nucleotides downstream. Symptoms of mutant 3′-Δ142–162-infected plants were similar to that shown by the plants infected with the WT TVBMV and the progeny mutant virus RNA maintained its original deletion (sequencing data not shown). According to the Mfold prediction, the deleted sequence did not affect the stem loop formation in the 3'-UTR (Fig. S1).

3.3. The 3′-UTR 5′-proximal stem loop structure is crucial for TVBMV systemic infection

According to the Mfold prediction, nucleotides (position 8–42) in the TVBMV 3′-UTR formed a stem loop (SL) like structure (Fig. 5A). This SL like structure was abolished after deleting nucleotides 1–20 (Fig. S2). When the progeny 3′-Δ1–20 mutant RNA sequences (Fig. 4B) were used for prediction, similar SL like structures were obtained (Fig. 5B and C). Similar results were also obtained for the progeny 3′-Δ8–14, 3′-Δ15–35 and 3′-Δ36–42 mutant virus. Because progeny of 3′-Δ15–35 mutant virus acquired 35 nucleotides at the original deletion site, the resulting SL like structure was longer than that in the WT TVBMV sequence (Fig. 5D). These findings imply that the SL like structure at nucleotide position 8–42 may have an essential role in TVBMV systemic infection.

To validate the above speculation, we produced two new constructs by inserting the acquired 14 nucleotides (atattatagtgtag, Fig. 4B) into the original deletion site in the parental mutant 3′-Δ1–20 to produce 3′-Δ1–20/14nt^{Ins} or the 35 nucleotides (atagtgtattgttgtttttctgtaccactagattat, Fig. 4B) into the original deletion site in the parental mutant 3′-Δ15–35 to produce 3′-Δ15–35/35nt^{Ins}. After infiltration of these two constructs into *N. benthamiana* plants, the plants showed systemic vein clearing symptoms and green fluorescence by 6 dpai. In contrast, plants infiltrated with the parental mutant 3′-Δ1–20 or 3′-Δ15–35 construct failed to show any virus like symptoms or green fluorescence by 6 dpai (Fig. 6A). Result of qRT-PCR showed that mutant 3′-Δ1–20/14nt^{Ins} or 3′-Δ15–35/35nt^{Ins} was able to accumulate in the systemic leaves of *N. benthamiana* plants by 6 dpai (Fig. 6B). Mutant 3′-Δ1–20 and 3′-Δ15–35 also accumulated in the systemic leaves of *N. benthamiana* plants by 11 dpai but their accumulation levels were only about 15% and 13% of the WT virus (Fig. 1C). Compared with their parental viruses, virus symptoms caused by mutant 3′-Δ1–20/14nt^{Ins} or 3′-Δ15–35/35nt^{Ins} were more severe. Sequence analyses showed that progeny 3′-Δ1–20/14nt^{Ins} and 3′-Δ15–35/35nt^{Ins} mutant viruses maintained their full length inserted sequences. These results indicated that the restored SL like structures were stable during virus replication and movement.

3.4. The 5'-end SL like structures of most potyviruses were conserved

In this study we also compared the 5'-end SL like structure in TVBMV 3′-UTR with that of other 11 potyviruses: *Tobacco vein mottling virus* (TVMV, X04083), *Potato virus Y* (PVY, MF440322), *Plum pox virus Y* (PPV, X16415), *Tobacco etch virus* (TEV, M11458), *Zucchini yellow mosaic virus* (ZYMV, AY278998), *Watermelon mosaic virus* (WMV, DQ399708), *Soybean mosaic virus* (SMV, HQ396725), *Sugarcane mosaic virus* (SCMV, JN021933), *Sweet potato feathery mottle virus* (SPFMV, AB465608), *Potato virus A* (PVA, Z21670), and ClYVV (AB01181) using the Mfold software. Results showed that the 5'-end SL like structures in TVBMV, TVMV, PVY, PPV, TEV, ZYMV, WMV, SMV and SCMV 3′-UTRs were similar, even though the sequences encompassing the 5'-end SL like structures sheared low sequence similarities among the nine viruses (Fig. S3). The 5'-end SL like structures in TVMV, PVY, SMV, WMV, and ZYMV 3′-UTRs were shorter than that in TVBMV, while the 5'-end SL like structures in PPV, SCMV and TEV 3′-UTRs were longer than that in TVBMV. The 5'-end SL like structures in SPFMV, PVA and ClYVV 3′-UTRs were quite different from that in TVBMV and no SL structure existed (Fig. S4).

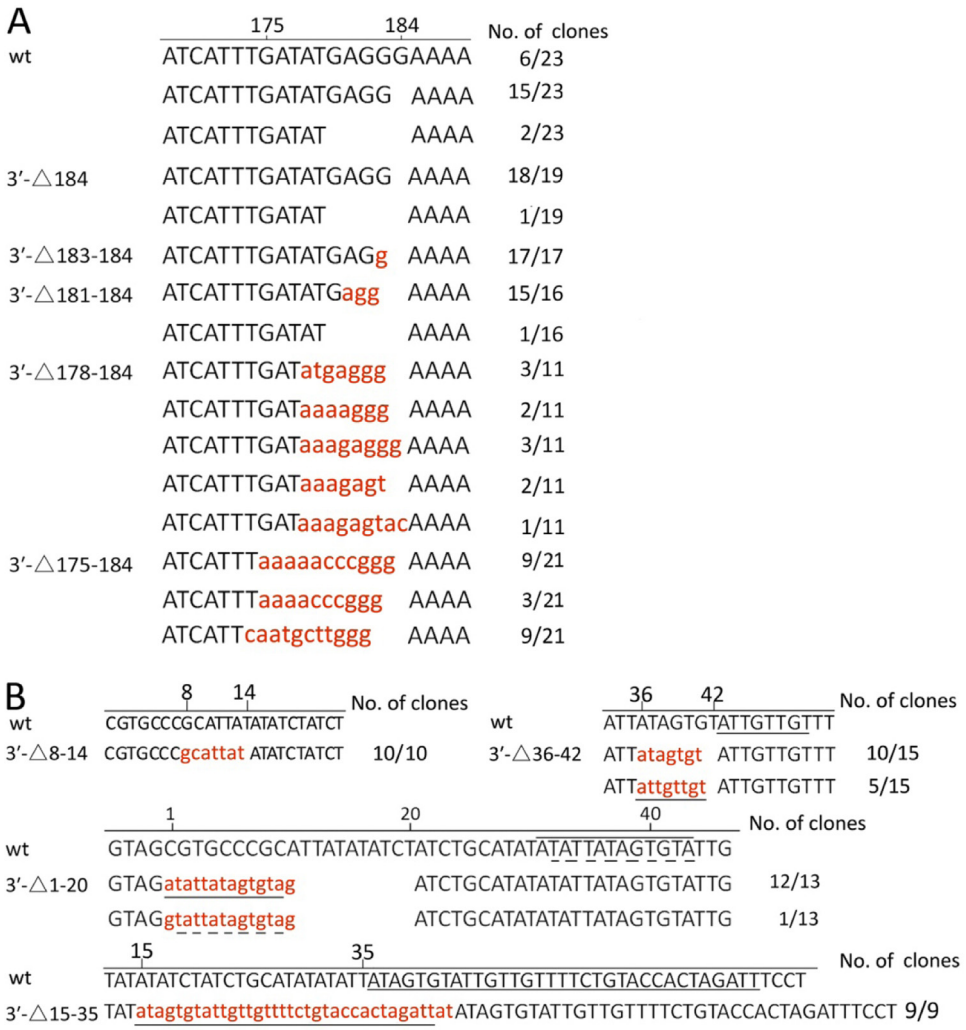

Fig. 4. 3′-UTR sequences of the progeny viral genome of WT TVBMV and deletion mutants. A, 3′-proximal sequence in the progeny viral genome of WT and 3′-terminal deletion mutants; B, The 5′-end sequences of 3′-UTR in the progeny viral genome of 3′-Δ1–20, 3′-Δ8–14, 3′-Δ15–35, and 3′-Δ36–42. Note: Lower case and colored nucleotides indicating the additional restored nucleotides at original deletion location.

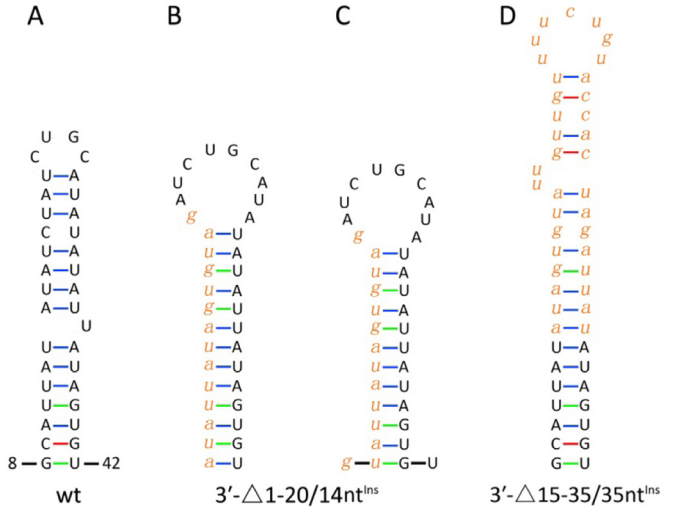

Fig. 5. RNA secondary structures of the 5′-end in 3′-UTR of the genomic RNAs of WT (A) and progeny viruses of 3′-Δ1–20 (B, C), 3′-Δ15–35(D). Note: lower-case and colored nucleotides indicating the additional restored nucleotides in the progeny RNA of different mutants.

4. Discussion

4.1. Two cis-acting elements in TVBMV 3′-UTR were crucial for TVBMV systemic infection

Here we report that inoculation of *N. benthamiana* plants with TVBMV mutants lacking different fragments in the 3′-UTR resulted in three different phenotypes. The first phenotype is represented by symptoms similar to that caused by the wild type TVBMV. For example, deletion of nucleotides from position 142–162 in the 3'-UTR, nucleotide 184, 183–184, or 181–184 had no significant effect on TVBMV systemic movement, pathogenicity, and viral RNA accumulation in infected plants (Figs. 2B, 3B), indicating that these deleted nucleotides are dispensable for TVBMV systemic infection. The second phenotype is represented by delayed virus systemic infection. For example, mutants with deletions at the nucleotide position 1–20 (3′-Δ1–20), 8–14 (3′-Δ8–14), 15–35 (3′-Δ15–35) and 36–42 (3′-Δ36–42) at the 5′-terminus, or 178–184 (3′-Δ178–184), 175–184 (3′-Δ175–184) at the 3′-terminus of 3′-UTR caused delayed systemic symptom development, milder vein clearing and mosaic symptoms, and less accumulation of viral RNA (Figs. 1B, 3B). Similar phenotype was also reported for plant-infecting *Brome mosaic virus* (BMV) RNA2 (Hema et al., 2005), CMV satellite RNA (Kwon et al., 2014; Sekiguchi et al., 2003), TCV satellite RNA C (Guan and Simon, 2000), *Beet necrotic yellow vein virus* (BNYVV) (Jupin et al.,

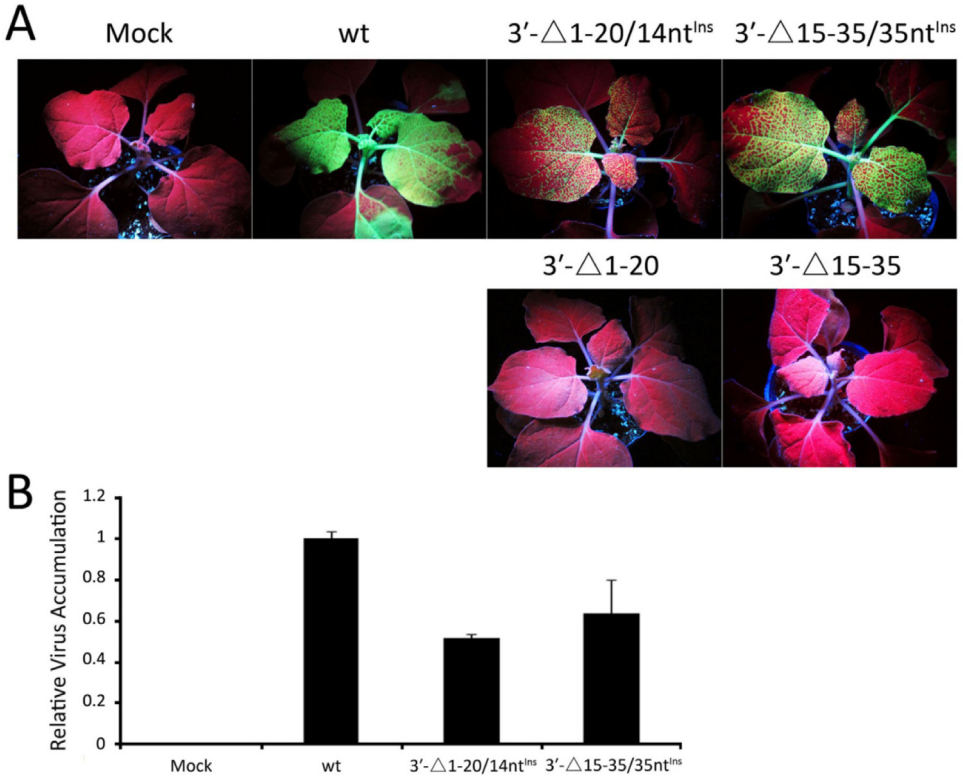

Fig. 6. Effect of 5′-terminal stem-loop structure in 3′-UTR on systemic movement of TVBMV. A, Green fluorescence detection in the *Nicotiana benthamiana* plants at 6 dpi under UV light ; B, Relative RNA accumulation in systemically infected leaves through qRT-PCR at 6 dpi.

1990), ClYVV (Tacahashi and Uyeda, 1999), and animals-infecting *Dengue virus* type 2 (Teramoto et al., 2008), *Hepatitis C virus* (van Leeuwen et al., 2006), and *Sindbis virus* (George and Raju, 2000). The third phenotype is represented by no systemic infection. For example, mutants with deletions at the nucleotide position 8–42 (3′-Δ8–42) close to the 5′-terminus; nucleotide position 43–60 (3′-Δ43–60), 61–100 (3′-Δ61–100), 101–141 (3′-Δ101–141) or 163–174 (3′-Δ163–174) in the middle region; nucleotide position 165–184 (3′-Δ165–184) at the 3′-terminus of the 3′-UTR abolished virus systemic infection (Figs. 1B, 2B and 3B). It is noteworthy that although deletion of nucleotide position 8–14 (3′-Δ8–14), 14–35 (3′-Δ14–35) or 36–42 (3′-Δ36–42) did not affect TVBMV systemic movement in *N. benthamiana* plants, deletion of nucleotide position 8–42 (3′-Δ8–42) abolished TVBMV systemic infection (Fig. 1B). Based on the above results, we conclude that nucleotide position 8–141 and 165–180 in the 3′-UTR contain *cis*-acting elements that are essential for TVBMV systemic movement in plant. A previous study had shown that the 5′-terminal 211 nt in the 3′-UTR of *Japanese encephalitis virus* (JEV) was dispensable for JEV infection, although the size of infectious foci or plaques caused by the mutants with deletions in this region was about 25% smaller than that caused by the wild type JEV. In contrast, the 3′-proximal domain II-2 or III were indispensable for JEV replication and accumulation (Yun et al., 2009). To further confirm the function(s) of 3′-UTR in TVBMV infection in plant, more studies on mutant virus cell-to-cell movement and/or replication in infected cells are needed.

4.2. Deletion in mutant virus can be repaired through nucleotide acquisition in vivo

RNA-dependent RNA polymerase of RNA virus has an error-prone nature. Therefore, genomes of RNA viruses are continuously under pressures to mutate, resulting in a quasispecies (Domingo, 2006). Of the 23 clones obtained from the WT TVBMV-inoculated *N. benthamiana* plants, 17 clones had changes in the 3′-UTR (Fig. 4A). This finding supports the above report that RNA virus changes constantly. On the other hand, numerous reports have indicated that RNA virus can efficiently repair their damaged sequences through various mechanisms (Teramoto et al., 2008; van Leeuwen et al., 2006). Template-independent addition of sequences was reported to be used by RNA viruses to repair their deleted sequences (Burgyan and Garcia-Arenal, 1998) or to restore the RNA structural integrity (Kwon et al., 2014). For *Dengue virus type* 2, deletions of longer sequences from viral genome caused slower virus systemic infection and the deletions were less likely to repaired (Teramoto et al., 2008). In this study, TVBMV mutants with one, two, or four nucleotide deletions were almost all repaired to form the WT sequence (Fig. 4A). Although mutants with seven or ten nucleotide deletion were also repaired but their repaired sequences were different from that of the WT virus and AG-rich (Fig. 4B). We speculate that the added nucleotides were randomly selected under the influence of the host plant. Because virus genomic RNAs with higher fitness have better compatibility during infection process, and thus may eventually become the predominant sequences in the virus population. In this study, although most progeny mutant virus were repaired, the progeny of WT virus still had better ability to replicate in cells and move between cells or between leaves.

In this study some sequences immediately downstream of the original deletion sites were copied into the deletion site (i.e., progeny of mutant 3′-Δ1–20, 3′-Δ8–14, 3′-Δ15–35 and 3′-Δ36–42 [Fig. 4B]). This finding is similar to that reported for JEV (Yun et al., 2009). Although how those sequences inserted into the original deletion sites in progeny mutant 3′-Δ1–20 or 3′-Δ15–35 is unknown, it is possible that the viral RNA polymerase paused at a site adjacent to the deletion site and then initiate polymerization again by duplicating the upstream sequences. For progeny mutant 3′-Δ8–14 and 3′-Δ36–42, viral polymerase may use parts of SL sequences as templates to repair the deletions.

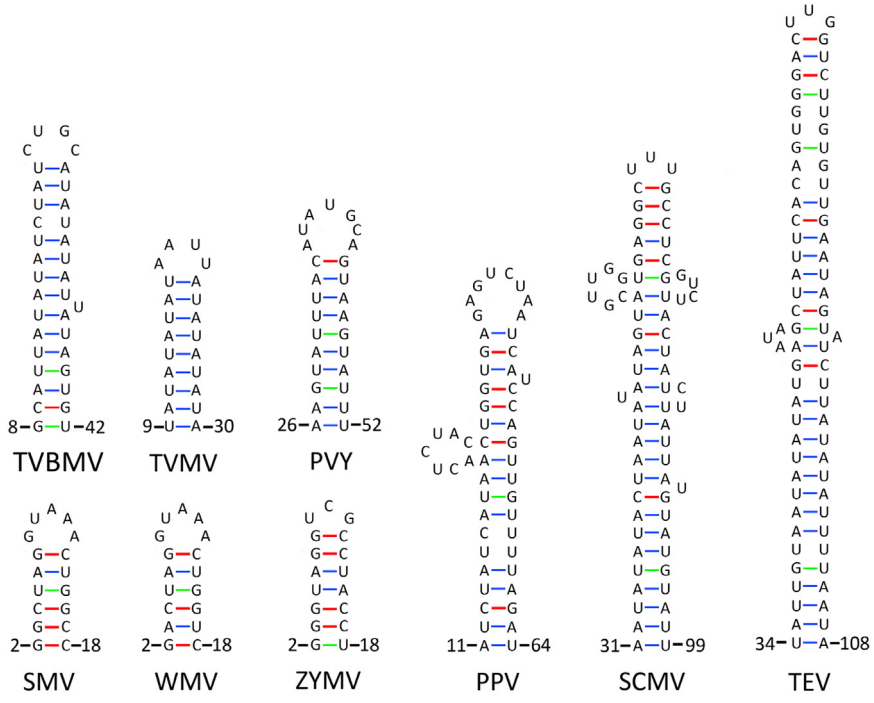

Fig. 7. Predicted secondary structure of the 5′-terminal sequence of 3′-UTR in members of the *Potyvirus*.

4.3. The SL like structure at the 5′-terminus of the 3′-UTR was crucial for TVBMV systemic infection

According to the prediction of RNA secondary structures, nucleotide at the position 8–42 can form a SL like structure (Fig. 5A). Because systemic infection caused by mutant virus: 3′-Δ1–20, 3′-Δ8–14, 3′-Δ15–35 and 3′-Δ36–42 was significantly delayed (Fig. 1), we propose that this 5'-terminal SL like structure is critical for TVBMV systemic infection. This speculation is supported by the fact that the 5'-terminal SL like structures in the progeny mutant 3′-Δ1–20 and 3′-Δ15–35 RNA were restored after acquiring additional nucleotides at the original deletion loci (Fig. 4B). Progeny mutant 3′-Δ1–20 and 3′-Δ15–35 virus with the restored 5'-terminal SL like structures have the ability to cause systemic infection in *N. benthamiana* plants, though less efficient than the WT TVBMV (Fig. 6A). Because similar SL like structures were also predicted in the 5'-terminal of the 3′-UTR of eight other potyviruses (Fig. 7), we speculate that the 5'-terminal SL like structure is indispensable for systemic infection of most potyviruses. A similar secondary structure was reported to be present in the 3′-end of CMV Q-satRNA and its mutant progeny virus with this secondary structure were capable of replicating in infected cells and causing systemic infection in its host plant (Gordon and Symons, 1983). Moreover, highly conserved SL like structures were recovered in the progeny RNAs from the systemic leaves infected with mutants of CMV satRNAs (Kwon et al., 2014). Taken together, the results presented in this paper extend our knowledge on the function of potyvirus 3′-UTR during virus infection in plant and on the mechanism controlling potyvirus pathogenicity in host plant.

Acknowledgement

This study was supported by grants from the National Natural Science Foundation of China (NSFC; 31571984, 31701760), and Funds of Shandong "Double Tops" Program.

Appendix A. Supporting information

Supplementary data associated with this article can be found in the online version at doi:10.1016/j.virol.2018.11.001.

References

Alvarez, D.E., De Lella Ezcurra, A.L., Fucito, S., Gamarnik, A.V., 2005. Role of RNA structures present at the 3'UTR of dengue virus on translation, RNA synthesis, and viral replication. Virology 339, 200–212.

Bienz, K., Egger, D., Pfister, T., Troxler, M., 1992. Structural and functional characterization of the poliovirus replication complex. J. Virol. 66, 2740–2747.

Bol, J.F., 2005. Replication of alfamo- and ilarviruses: role of the coat protein. Annu. Rev. Phytopathol. 43, 39–62.

Burgyan, J., Garcia-Arenal, F., 1998. Template-independent repair of the 3' end of cucumber mosaic virus satellite RNA controlled by RNAs 1 and 2 of helper virus. J. Virol. 72, 5061–5066.

Chung, B.Y., Miller, W.A., Atkins, J.F., Firth, A.E., 2008. An overlapping essential gene in the *Potyviridae*. Proc. Natl. Acad. Sci. USA 105, 5897–5902.

Cui, W., Liu, W., Wu, G., 1995. A simple method for the transformation of *Agrobacterium tumefaciens* by foreign DNA. Chin. J. Biotechnol. 11, 267–274.

Domingo, E., 2006. Quasispecies: concepts and implications for virology. Curr. Top Microbiol Immunol 299 Springer-Verlag, Berlin Heidelberg.

Dong, Y., Yang, J., Ye, W., Wang, Y., Miao, Y., Ding, T., Xiang, C., Lei, Y., Xu, Z., 2015. LSm1 binds to the dengue virus RNA 3' UTR and is a positive regulator of dengue virus replication. Int. Iournal Mol. Med. 35, 1683–1689.

Dreher, T.W., 2009. Role of tRNA-like structures in controlling plant virus replication. Virus Res. 139, 217–229.

Gao, R., Tian, Y.P., Wang, J., Yin, X., Li, X.D., Valkonen, J.P., 2012. Construction of an infectious cDNA clone and gene expression vector of *Tobacco vein banding mosaic virus* (genus *Potyvirus*). Virus Res. 169, 276–281.

Garnier, M., Candresse, T., Bove, J.M., 1986. Immunocytochemical localization of TYMV-coded structural and nonstructural proteins by the protein A-gold technique. Virology 151, 100–109.

Geng, C., Cong, Q.Q., Li, X.D., Mou, A.L., Gao, R., Liu, J.L., Tian, Y.P., 2015. Developmentally regulated plasma membrane protein of *Nicotiana benthamiana* contributes to potyvirus movement and transports to plasmodesmata via the early secretory pathway and the actomyosin system. Plant Physiol. 167, 394–410.

George, J., Raju, R., 2000. Alphavirus RNA genome repair and evolution: molecular characterization of infectious sindbis virus isolates lacking a known conserved motif at the 3' end of the genome. J. Virol. 74, 9776–9785.

Gordon, K.H., Symons, R.H., 1983. Satellite RNA of cucumber mosaic virus forms a secondary structure with partial 3'-terminal homology to genomal RNAs. Nucleic Acids Res. 11, 947–960.

Guan, H., Simon, A.E., 2000. Polymerization of nontemplate bases before transcription initiation at the 3' ends of templates by an RNA-dependent RNA polymerase: an activity involved in 3' end repair of viral RNAs. Proc. Natl. Acad. Sci. USA 97, 12451–12456.

Guo, S., Wong, S.M., 2018. Disruption of a stem-loop structure located upstream of pseudoknot domain in Tobacco mosaic virus enhanced its infectivity and viral RNA accumulation. Virology 519, 170–179.

Hema, M., Gopinath, K., Kao, C., 2005. Repair of the tRNA-like CCA sequence in a multipartite positive-strand RNA virus. J. Virol. 79, 1417–1427.
Iwakawa, H.O., Kaido, M., Mise, K., Okuno, T., 2007. cis-Acting core RNA elements required for negative-strand RNA synthesis and cap-independent translation are separated in the 3'-untranslated region of R*ed clover necrotic mosaic virus RNA1*. Virology 369, 168–181.
Jupin, I., Bouzoubaa, S., Richards, K., Jonard, G., Guilley, H., 1990. Multiplication of beet necrotic yellow vein virus RNA 3 lacking a 3′ltiplication of beet necrotic yellow vein vir of the poly (A) tail and a novel short U-rich tract preceding it. Virology 178, 281–284.
Kwon, S.J., Chaturvedi, S., Rao, A.L., 2014. Repair of the 3' proximal and internal deletions of a satellite RNA associated with *Cucumber mosaic virus* is directed toward restoring structural integrity. Virology 450–451, 222–232.
Liu, H., Naismith, J.H., 2008. An efficient one-step site-directed deletion, insertion, single and multiple-site plasmid mutagenesis protocol. BMC Biotechnol. 8, 91.
Mackenzie, J.M., Khromykh, A.A., Jones, M.K., Westaway, E.G., 1998. Subcellular localization and some biochemical properties of the flavivirus Kunjin nonstructural proteins NS2A and NS4A. Virology 245, 203–215.
Schmittgen, T.D., Zakrajsek, B.A., Mills, A.G., Gorn, V., Singer, M.J., Reed, M.W., 2000. Quantitative reverse transcription-polymerase chain reaction to study mRNA decay: comparison of endpoint and real-time methods. Anal. Biochem. 285, 194–204.
Sekiguchi, H., Tacahashi, Y., Uyeda, I., 2003. The 3' terminal region is strictly required for clover yellow vein virus genome replication. Arch. Virol. 148, 759–772.
Shwetha, S., Kumar, A., Mullick, R., Vasudevan, D., Mukherjee, N., Das, S., 2015. HuR displaces polypyrimidine tract binding protein to facilitate La binding to the 3' untranslated region and enhances hepatitis C Virus replication. J. Virol. 89, 11356–11371.
Skuzeski, J.M., Bozarth, C.S., Dreher, T.W., 1996. The turnip yellow mosaic virus tRNA-like structure cannot be replaced by generic tRNA-like elements or by heterologous 3' untranslated regions known to enhance mRNA expression and stability. J. Virol. 70, 2107–2115.
Tacahashi, Y., Uyeda, I., 1999. Restoration of the 3' end of potyvirus RNA derived from Poly(A)-deficient infectious cDNA clones. Virology 265, 147–152.
Teramoto, T., Kohno, Y., Mattoo, P., Markoff, L., Falgout, B., Padmanabhan, R., 2008. Genome 3'-end repair in dengue virus type 2. RNA 14, 2645–2656.
Tian, Y.P., Liu, J.L., Yu, X.Q., Lei, L.P., Zhu, X.P., Valkonen, J.P., Li, X.D., 2007. Molecular diversity of tobacco vein banding mosaic virus. Arch. Virol. 152, 1911–1915.
van Leeuwen, H.C., Liefhebber, J.M., Spaan, W.J., 2006. Repair and polyadenylation of a naturally occurring hepatitis C virus 3rnontranslated region-shorter variant in selectable replicon cell lines. J. Virol. 80, 4336–4343.
Winer, J., Jung, C.K., Shackel, I., Williams, P.M., 1999. Development and validation of real-time quantitative reverse transcriptase-polymerase chain reaction for monitoring gene expression in cardiac myocytes in vitro. Anal. Biochem. 270, 41–49.
Yun, S.I., Choi, Y.J., Song, B.H., Lee, Y.M., 2009. 3' cis-acting elements that contribute to the competence and efficiency of Japanese encephalitis virus genome replication: functional importance of sequence duplications, deletions, and substitutions. J. Virol. 83, 7909–7930.
Zuker, M., 2003. Mfold web server for nucleic acid folding and hybridization prediction. Nucleic Acids Res. 31, 3406–3415.